Scanning Electron Probe Microanalysis

M. Vijayakumar, V.V. Rama Rao and P.C. Angelo*

Defence Metallurgical Research Laboratory, Hyderabad–500 258

ABSTRACT

Scanning electron probe microanalysis has grown over the past three decades into a powerful technique for the microchemical characterisation of materials. This paper describes the principles and various features of a typical microanalyser, and illustrates its unique capabilities in the study of materials by means of selected case histories.

1. INTRODUCTION

Electron Probe Microanalysis (EPMA) has emerged in the past three dacades as a unique technique for the microchemical characterisation of materials. It has its experimental beginnings in the work of Moseley[1] who in 1913 discovered the general relationship between the x-ray emission lines of an element and its atomic number and indicated the possibility of chemical analysis by examination of the x-ray emission spectrum of a material generated by electron bombardment. It was not until 1949, however, that this proposal was explored further by Castaing and Guinier[2] who described an instrument called electron microprobe for this purpose. In his doctoral thesis in 1951, Castaing[3] presented the details of the instrument they had built along with a sound theoretical formulation for quantitative chemical analysis. Cosslet and Duncumb[4] added electron beam scanning capability to such an equipment thus extending its versatility. The principal aspects of an 'electron probe microanalyser' remains essentially the same even today, though the tremendous advances made in the fields of electronics and instrumentation have contributed a great deal in improving the operational efficiency of such instruments. Present generation computer-controlled electron microprobes can perform the quantitative determination of a dozen elements in a material in a matter of minutes, once calibrated, without any operator intervention.

The electron probe microanalyser works on the following principle. The material under investigation is bombarded with a beam of electrons having energy sufficient enough to knock-out electrons from the inner orbitals of the atoms comprising the material. The core-shell vacancy thus created will be filled by the falling of an electron from one of the outer orbitals into this vacancy. The difference in energy between the outer shell electron and the core-shell vacancy is emitted out as an x-ray photon. The energy of this x-ray photon is characteristic of the atom emitting it, and the number of such photons emitted bears a relationship to the total number of atoms emitting them. In other words, qualitative and quantitative chemical information about the material can be obtained by the analysis of energy and intensity of the x-ray emission lines of the material. As an electron beam can be focussed by an electromagnetic field to a fine spot of less than 1 μm diameter, this technique finds unique applications in the study of micrometric level concentration gradients particularly at phase boundaries, surfaces, grain boundaries, diffusion couple interfaces, and welded sections; in the identification of inclusions and phases; in the determination of composition variation within a single phase (segregation); and in the identification of contaminants, both foreign to and characteristic of the material. In essence, this technique can be used in any application where chemical characterisation of a microfeature of the order of a micron is required, be it metallurgical, geological, agricultural, biological or lunar sample.

2. EXPERIMENTAL TECHNIQUE

Scanning electron probe microanalyser CAMEBAX-MICRO installed at Defence Metallurgical Research Laboratory (DMRL), Hyderabad, is an electron microprobe with an optical and secondary electron microscope for sample observation and imaging, a programmable microprocessor-controlled wavelength dispersive type x-ray analyser system for chemical analysis, and a PDP 11/03 minicomputer for fast data acquisition and processing. A schematic diagram of the electron microprobe is presented in Fig. 1. Various features of CAMEBAX-MICRO are presented in Table 1.

Major aspects of study using an electron microprobe are qualitative analysis, x-ray mapping and line profiling and quantitative analysis. For qualitative analysis of a material, all the three spectrometers are scanned simultaneously and the x-ray count data for each crystal position is acquired and stored in the computer. The elements corresponding to the crystal positions for which the count rate crosses a threshold level are then assorted by software and printed out on an LA-120 Decwriter terminal. A typical computer output for the qualitative analysis of a nickel-base alloy is presented in Appendix A. The x-ray spectral data acquired can also be presented graphically as a plot of crystal position in sine theta units against count rate for visual identification of the peaks as shown in Fig. 2. The elements indicated by this program can further be confirmed by checking if the x-ray count rate at the peak of an element is significantly different from that of the background. Such an analysis for a nickel-base alloy is shown in Appendix B. Software-controlled comprehensive qualitative analysis carried out in this manner takes about 10–20 minutes.
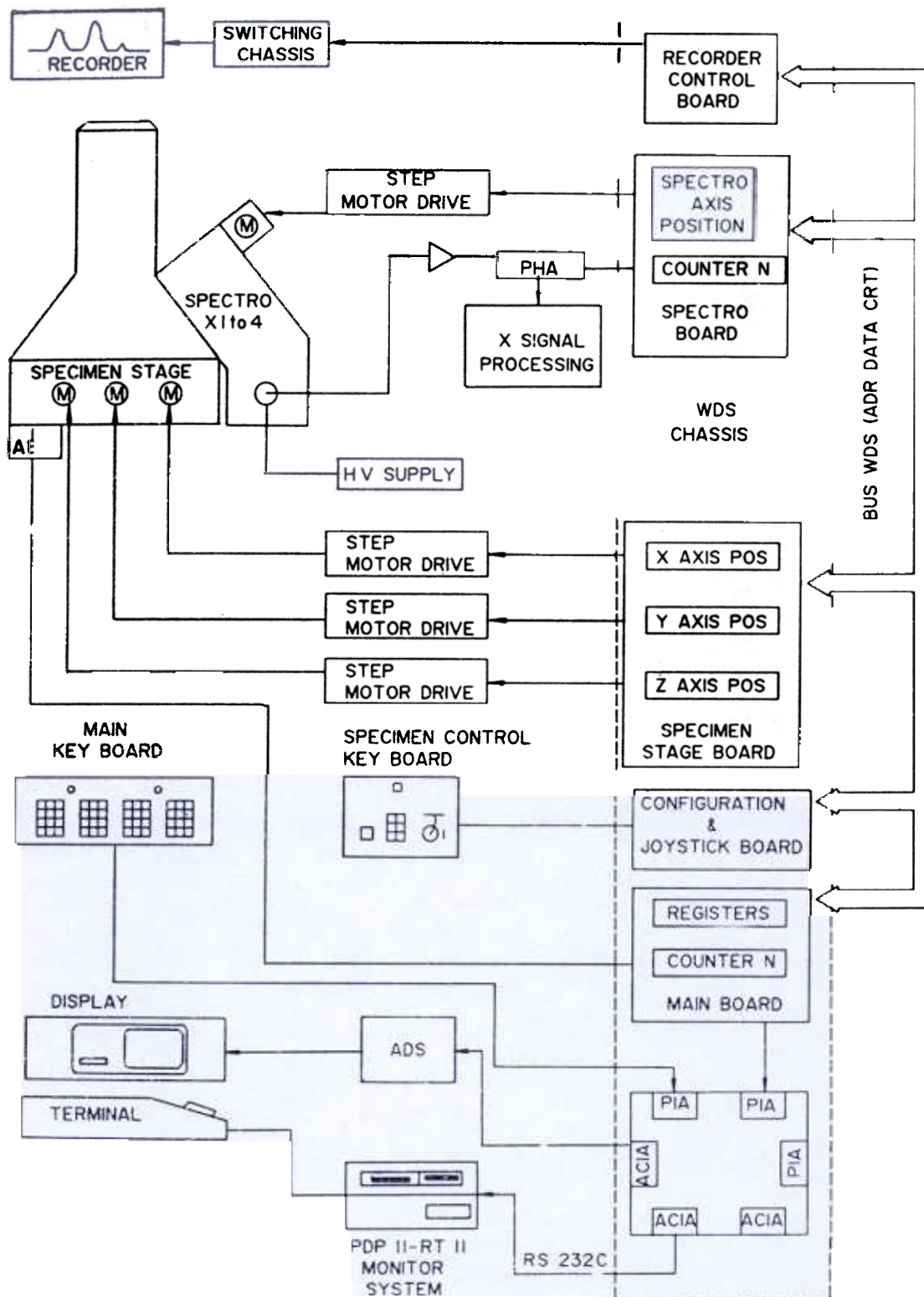
Figure 1. Schematic diagram of CAMEBAX-MICRO.

X-ray mapping and line profiling are the most widely used features of an electron microprobe analysis. In the former, the electron beam is rastered over an area on the sample and the x-ray signal for any given element of interest is used to modulate the dot-brightness of a synchronously scanning Cathode Ray Tube (CRT). In line profiling, the electron beam is scanned along a line on the sample and the x-ray signal generated

Table 1. CAMEBAX-MICRO scanning electron probe microanalyser at a glance

1. Optical microscope with a magnification of 400 (fixed) for sample observation.

2. Secondary electron and absorbed current imaging facility with magnification of 100 to 80 K, and separate CRTs for viewing and photographing images.

.3. Beam regulation device for keeping the electron beam current irradiating the sample constant.

4. Automated vacuum system (rotary and diffusion pump) providing a column vacuum of $>10^{-5}$ torr.

5. Microprocessor-controlled wavelength dispersive system.

6. One inclined and two vertical spectrometer configuration.

7. LIF, PET, TAP and ODPb crystals to cover the complete wavelength range for elements from boron to uranium.

8. Continuous flow argon–10 per cent methane gas proportional counter detector for x-rays.

9. Wide-field x-ray imaging and linescan facility for scanning upto 1000 μm.

10. HP recorder for plotting of microprocessor data.

11. PDP 11/03L minicomputer with 32 k words memory.

12. Software for qualitative and quantitative analyses including data acquisition and processing.

13. HP 7221C 8-pen plotter for offline plotting of x-ray spectrum, concentration profiles, mapping, etc., using PDP minicomputer.

is used to modulate the *y*-amplitude of a synchronously scanning CRT. Normally, the spectrometers do not remain in focus when the electron beam moves more than 50 μm from the centre of the scanned region during x-ray mapping or line profiling. In Camebax-Micro, this problem has been overcome by dynamic focussing of the spectrometers wherein the analysing crystal is moved synchronously with the electron beam, and mapping of regions as large as 1 square mm can be done; however, this can be achieved only in one specific direction in the plane of the specimen surface. Figure 3 shows a typical example of the x-ray distribution images obtained for a pack-siliconised *Ni-Al-Mo* eutectic alloy, while Fig. 4 presents the x-ray linescans to confirm the presence of titanium oxycarbides along the prior particle boundaries of a hot isostatically pressed nickel-base alloy prepared starting from powders.

For quantitative analysis, appropriate crystals are positioned in the spectrometers, and a standard calibration routine is run. The electron beam is focussed on pure elemental or compound standards, and the x-ray count rates for these standards are acquired and stored in the computer. The beam is then positioned on a selected region of the sample to be analysed, and the count rate for various elements acquired and stored in the computer.

The ratio of the count rates for an element in the sample to that of pure element is called *k*-ratio, and this quantity, to a first approximation gives the concentration of the element in the sample. However, there is a need to correct this concentration as the behaviour of x-rays and electrons are different in each material, causing the behaviour in an unknown material to differ from that in a standard.

When a material is bombarded with a beam of electrons, a part of the intensity is lost as a result of the backscattering of the electrons from the sample. To the extent
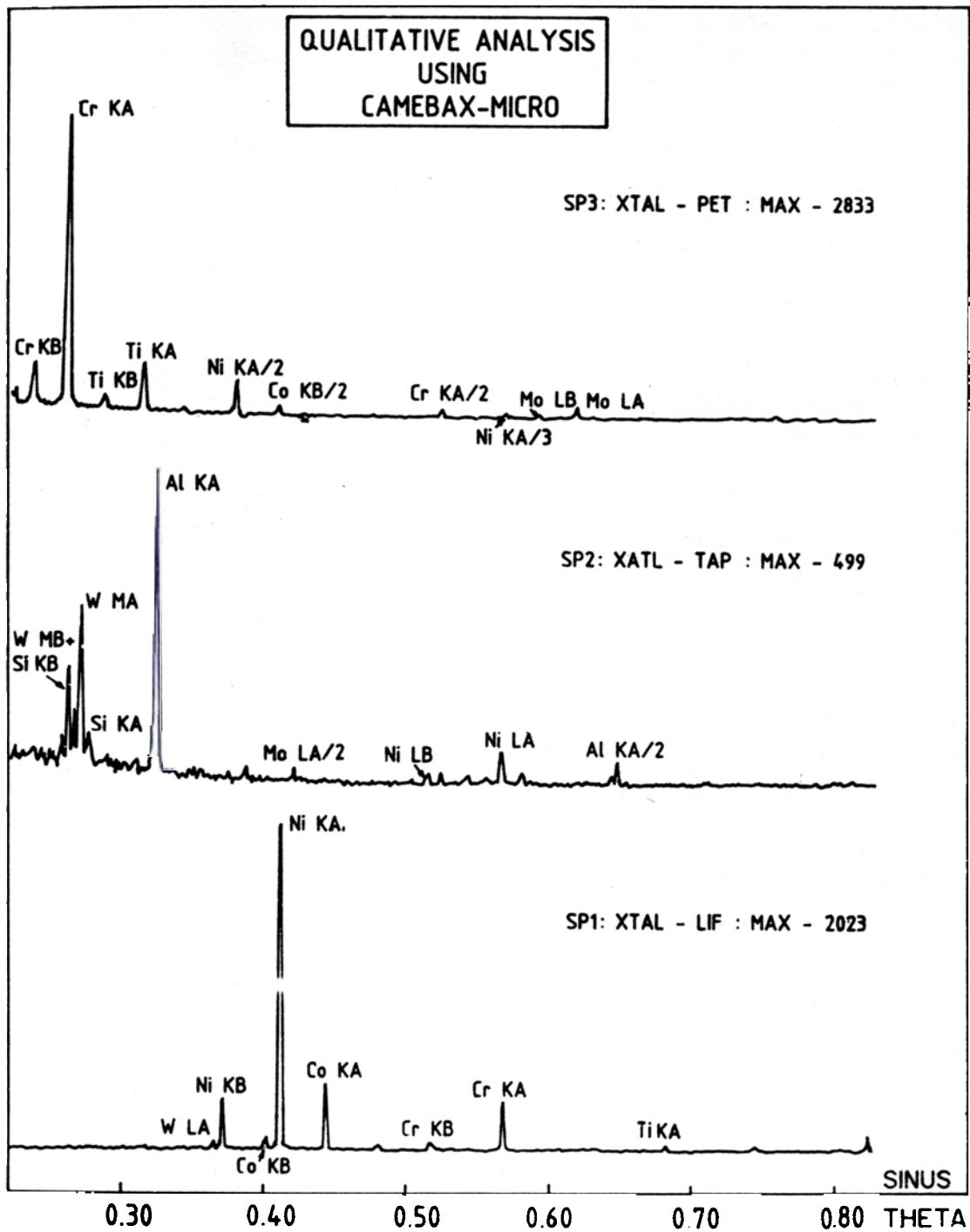
Figure 2.   X-ray spectrum of a Ni-base alloy.

that these electrons have energies in excess of the excitation potential of the element analysed, there is a loss of generated x-rays. And the extent of backscattering depends on the atomic number of the element. Also, as the electron beam penetrates the material, it loses its energy as a result of inelastic scattering. The depth distribution of the energy of the electrons is different in different materials and so is the distribution of x-rays generated as a result of inelastic scattering. The correction required to be made because of the backscattering as well as energy loss factor is called the atomic number (Z) correction.
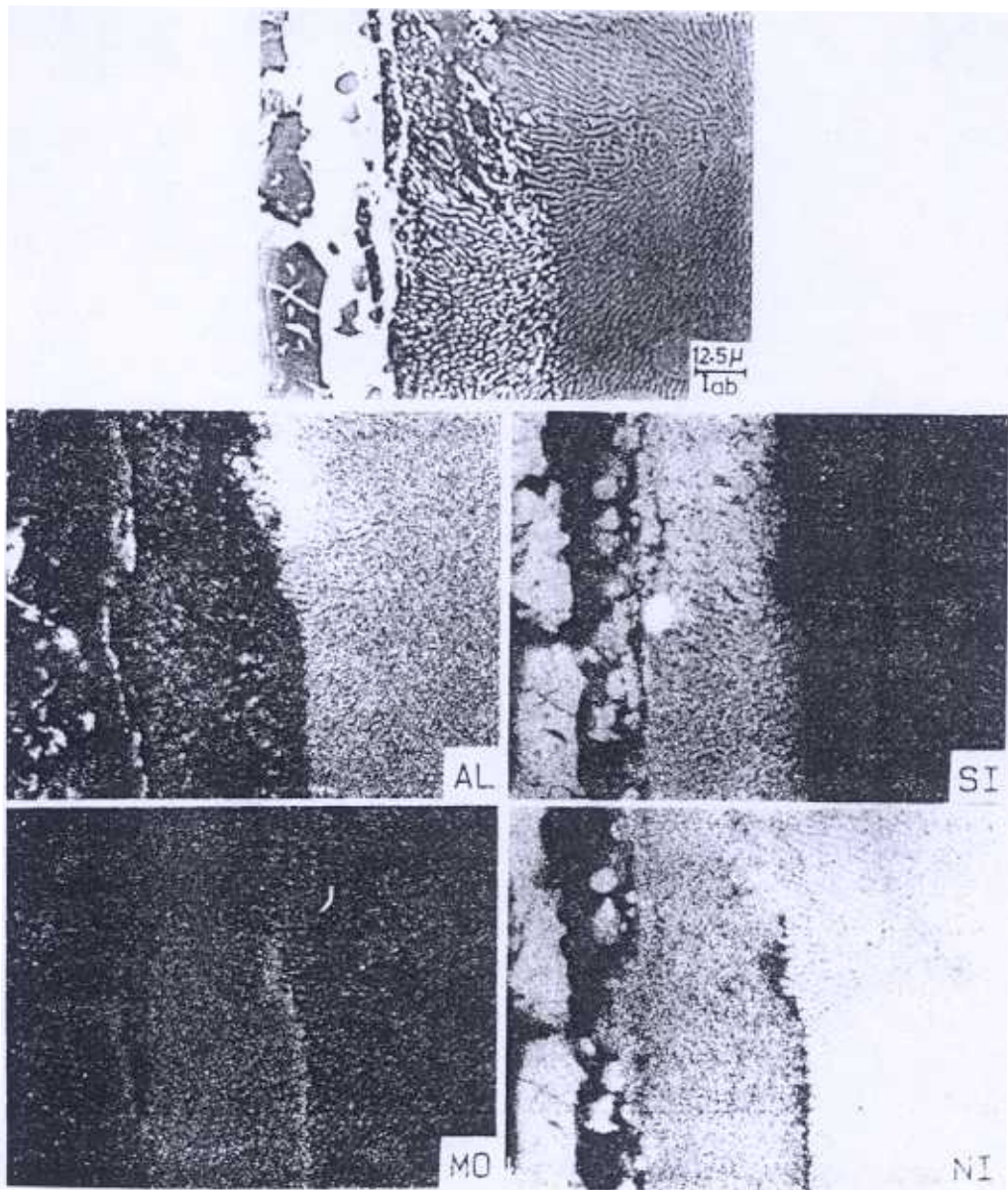
Figure 3.   X-ray elemental distribution images

X-rays generated along the depth of the material being analysed have to traverse through different distances in the material itself. Their intensity is thus attenuated because of absorption path length, the composition of the material intervening between the origin of the x-ray photon and the surface of the material, and the energy of the photon itself. The correction resulting from this factor is called the absorption (A) correction.

X-rays of one element can excite x-rays of another element present in the material being analysed. In such a case, the measured x-ray intensity will be more than what is actually generated by electron beam excitation only. The correction arising from this is called the flourscence (F) correction.

Excellent models for the calculation of the correction factors Z, A and F from the k-ratios of the elements in the material are available[5,6]. In Camebax-Micro this correction is done online using the PDP computer based on a COR 2 ZAF correction
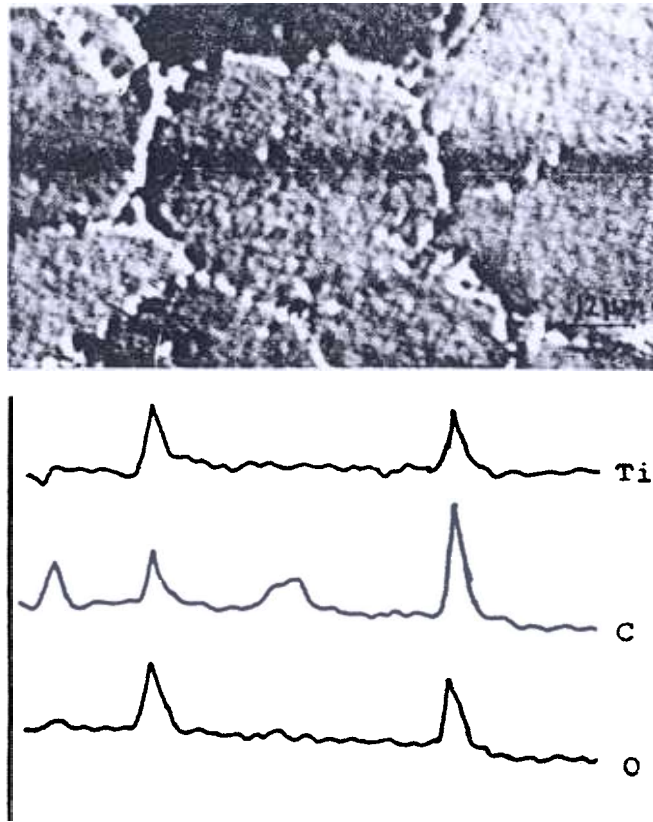
Figure 4. X-ray linescans.

program written by US National Bureau of Standards. The results of an online quantitative analysis for a magnetic alloy is presented in Appendix C. Once the count rate data for the standards is stored in the computer, the whole analysis for a dozen elements including the acquisition of count rate for all the elements in the sample, and correction takes about 10–15 minutes. As there is a beam regulation device to keep the electron beam current falling on the sample constant, a large number of points can be analysed without going back to the standards to check if their count rates have changed. It may be noted here that an accuracy of 1–5 per cent and a volume resolution of 2–5 μm^3 is achieved in this technique, the former being limited by the various simplifying assumptions and inaccuracies in the parameters used in the correction procedures, while the latter is limited by electron diffusion inside the material.

3. APPLICATIONS

All applications of electron probe microanalyser are centred around the fact that the chemical information provided by the microprobe is different from the one provided by wet chemical or instrumental techniques such as atomic absorption or plasma emission spectrometry. The former is responsive to the chemistry or regions of the order of a micron with a lateral as well as depth resolution of about a micron, while the latter essentially give the bulk composition of the material. While it is true that the lateral resolution of techniques such as Auger electron spectroscopy or secondary ion mass spectrometry is of the same order (or better) as that of the microprobe, the

information depth is limited to the first few atomic layers from the surface of the material. Thus analysis provided by microprobe is a via media between the two extremes of surface analysis and bulk analysis, and hence its uniqueness. An additional advantage of microprobe analysis is its non-destructive nature, though in some cases the sample preparation required or the electron beam-induced damage or transformation of the material under study may offset this.

At DMRL, the electron microprobe technique has been successfully utilised to solve many a metallurgical problem in connection with the development of special alloys for Defence hardware application and failure analysis of materials during service. A few case histories illustrating these aspects are presented in the following paragraphs.

3.1 Identification of Inclusions

The study of non-metallic inclusions in ferrous and non-ferrous alloys is of fundamental importance in understanding their formation and in evaluating the properties of the alloys vis-a-vis their microstructure. EPMA is the most extensively used technique to study the chemical nature of such inclusions. Two typical examples of inclusions in mild steel indentified by electron microprobe are shown in Figs. 5(a) and 5(b). The figures show the secondary electron and x-ray distribution images for various elements. The distribution of silicon, manganese and oxygen in Fig. 5(a) clearly delineates the existance of manganese silicate and silica phases in the duplex inclusion. Figure 5(b), on the other hand, is an example of a complex polyphase inclusion in steels.

## 3.2 Failure Analysis of a Steel Bolt

Electron microprobe has been successfully used in the course of an investigation on the failure of an EN-24 type steel bolt subjected to shock-loading. The fracture surface of the failed bolt exhibited secondary intergranular cracks as well as pits. Metallographic examination of the material showed the presence of a network structure all along the threaded region. Electron microprobe studies of the regions near the threaded portions showed the presence of inclusion, [Fig. 6(a)] which were identified from the x-ray elemental distribution maps [Fig. 6(b)] to be chromium oxide particles present along the grain boundaries. It was concluded that such oxidation along the grain boundaries could have taken place only during heat treatment. Based on this information, the recurrence of such failures was successfully avoided by carrying out the heat treatment under controlled atomosphere so as to eliminate the deleterious grain boundary oxidation.

3.3 Characterisation of Coatings

Considerable developments have taken place in the area of coatings to improve the performance of engineering alloys so as to enhance their resistance to wear, erosion, oxidation and corrosion The characterisation of such coatings as well as the interface between the coating and the substrate after heat treatment can be carried out by EPMA. Figure 7 shows a typical example of EPMA study of the
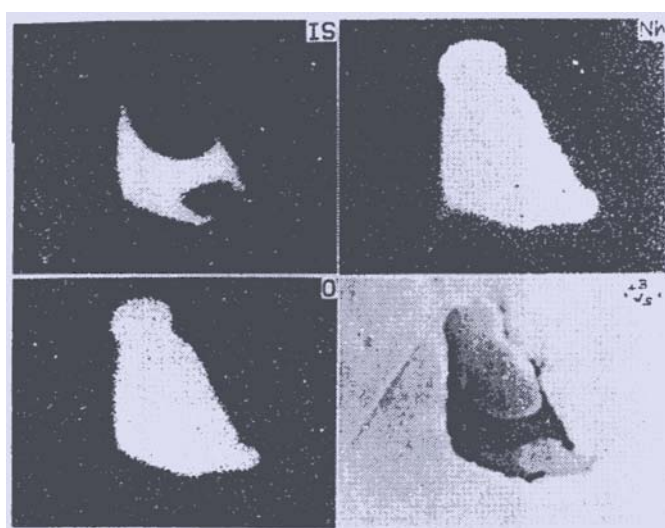
(a)
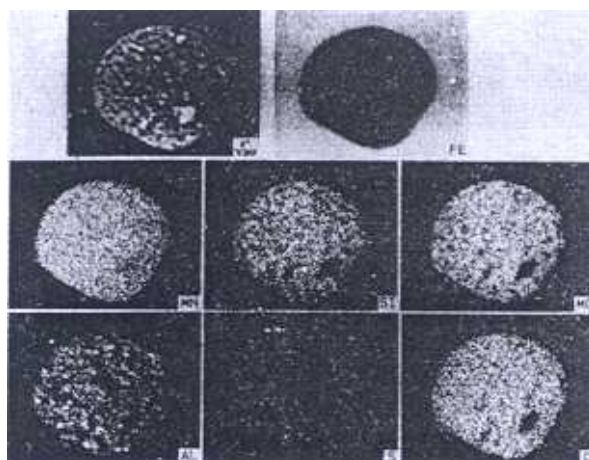
(b)

Figure 5. Inclusions in steel.

coating-substrate interface of a tungsten carbide-cobalt composite coating deposited by plasma-spraying on a mild steel substrate. The x-ray intensity variation across the substrate-coating interface taken along the line shown in the absorbed current image is given in Fig. 7. Quantitative analysis was also carried out at various discrete points along the linescan, and the results are also given in the Fig. 7. It can be clearly seen from the EPMA results that in the heat treated sample, cobalt gets depleted on the coating side while getting enriched on the substrate side of the interface. This indicates the formation of a reaction zone near the coating-substrate interface formed as a result of the heat treatment carried out for one hour at 1100°C in a vacuum of $>10^{-4}$ torr. Also, on the coating side, tungsten concentration remains constant, suggesting the possibility of the presence of a compound. In fact, x-ray diffraction analysis carried out on the sample, after removing the surface layers, indicated the presence of Co_6W_6C type of compound. (As the x-ray intensity profile for iron is complementary to that of cobalt on the coating side, iron might have replaced part of Co in this compound). The presence of a reaction zone, around the interface clearly explains the remarkable improvement in adhesion of the coating with the substrate on heat treatment.

M Vijayakumar, et al
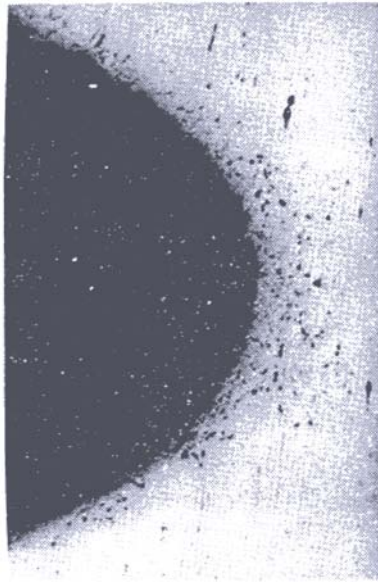
(a)
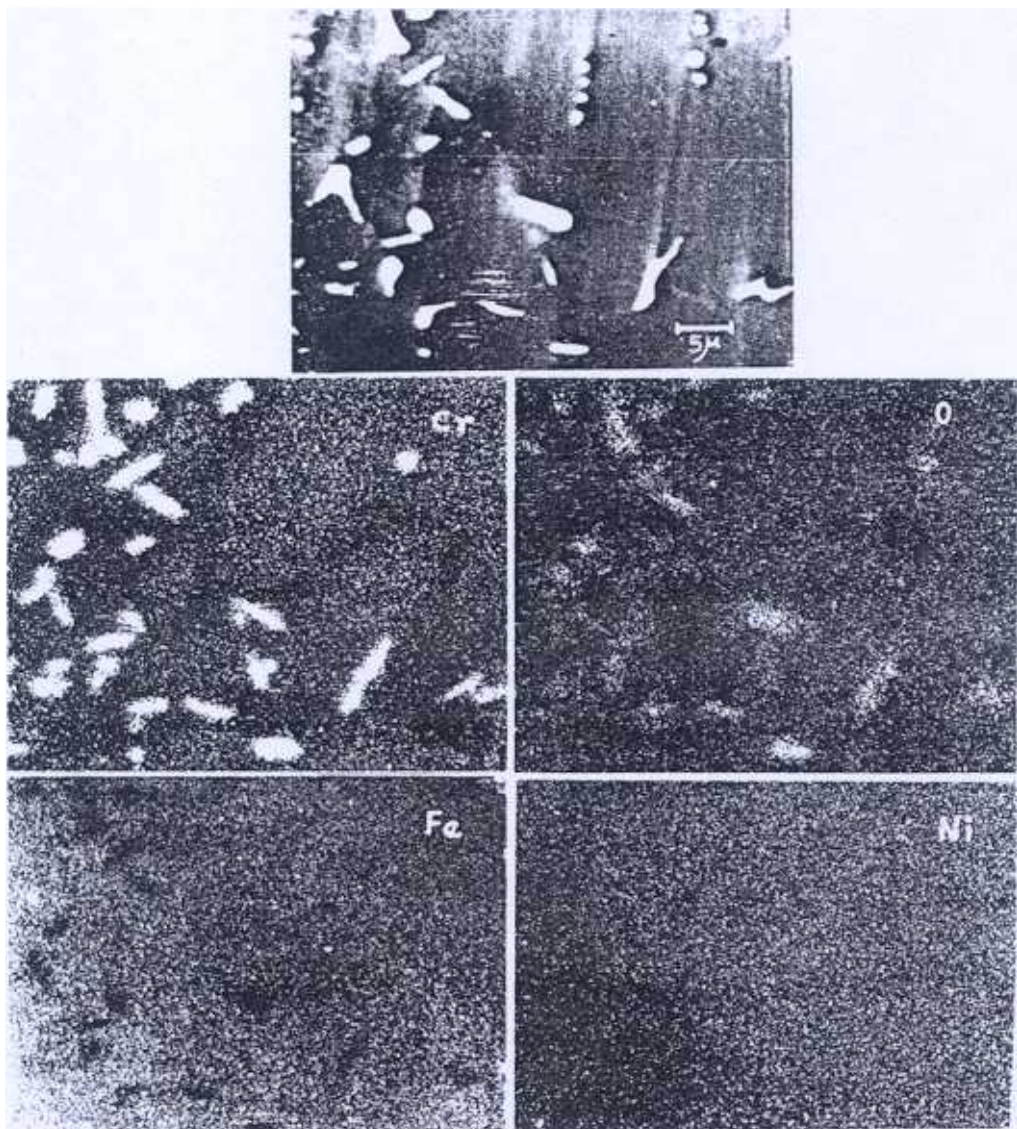
(b)

Figure 6. Studies in failure analysis : (a) optical micrograph, and (b) x-ray dot maps
of a threaded region.

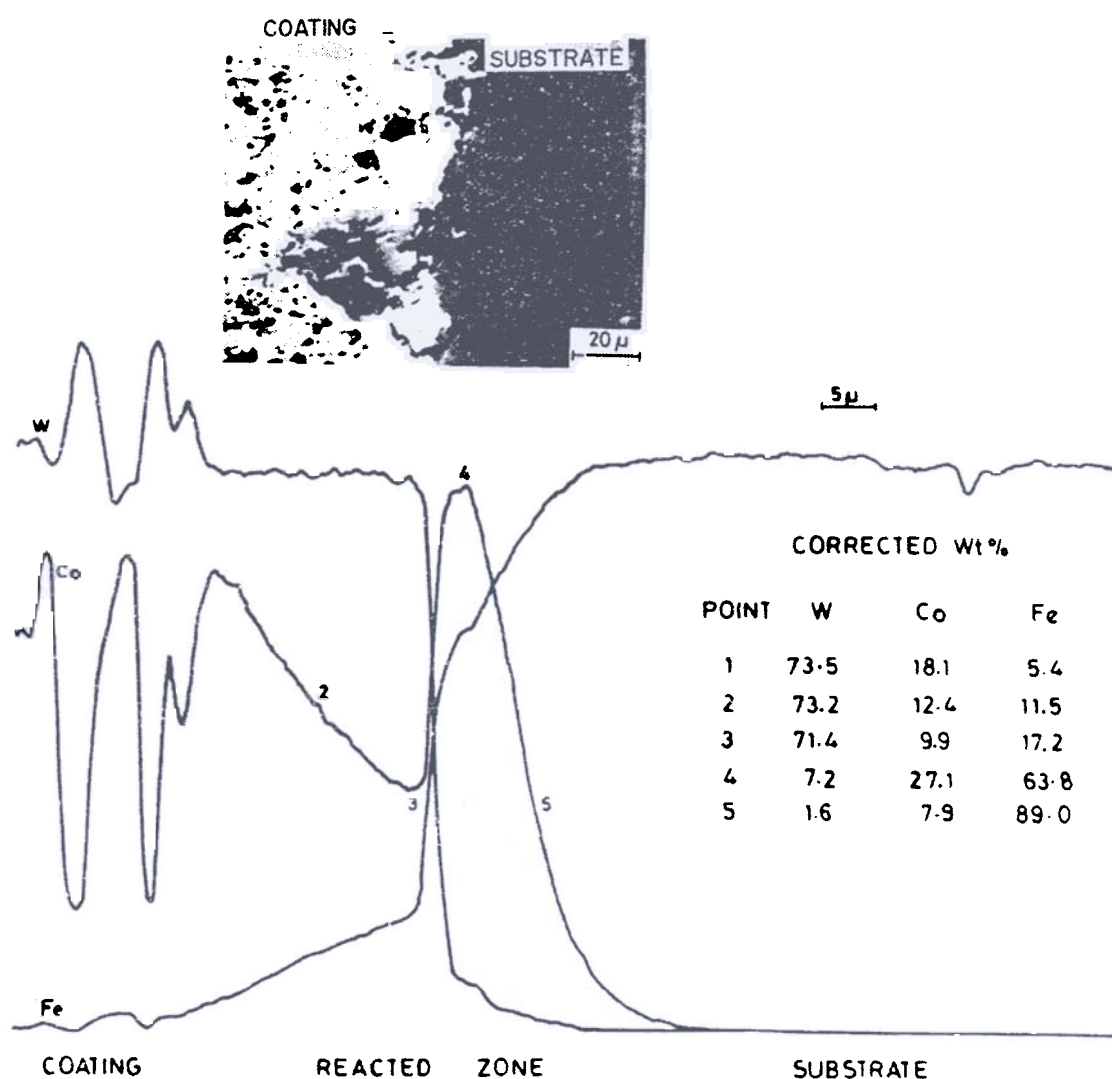| POINT	W	Co	Fe
1	73·5	18.1	5.4
2	73.2	12·4	11.5
3	71.4	9.9	17.2
4	7·2	27.1	63·8
5	1·6	7·9	89·0

Figure 7. Study of coatings.

3.4 Application to Mechanical Alloying

Metals and alloys having a fine distribution of insoluble hard particles show improved mechanical properties and microstructural stability at higher temperatures than those strengthened by precipitation or by solute additions. The normal method of producing oxide dispersion-strengthened alloys is either by internal oxidation or by chemical co-reduction. However, in recent years a powder metallurgical technique called 'mechanical alloying' is gaining importance. Mechanical alloying uses a high energy ball mill called 'attritor' to transform powder mixtures into homogeneous composite particles. At DMRL, the technique of mechanical alloying of nickel with chromium (20 wt. per cent) and thoria (2 per cent by volume) has been successfully carried out in a specially designed and fabricated attritor. Experiments have also been conducted to test the efficiency of a conventional ball mill for mechanical alloying. EPMA studies were conducted on the samples prepared by conventional ball milling as well as by the attritor. Results from EPMA proved decisively the inability of a conventional ball mill for mechanical alloying of chromium with nickel even after 90 hours of milling time [Fig. 8(a)]. However, the attritor easily enables homogeneous alloying of chromium with nickel in about 40 hours as seen in Fig. 8(b).
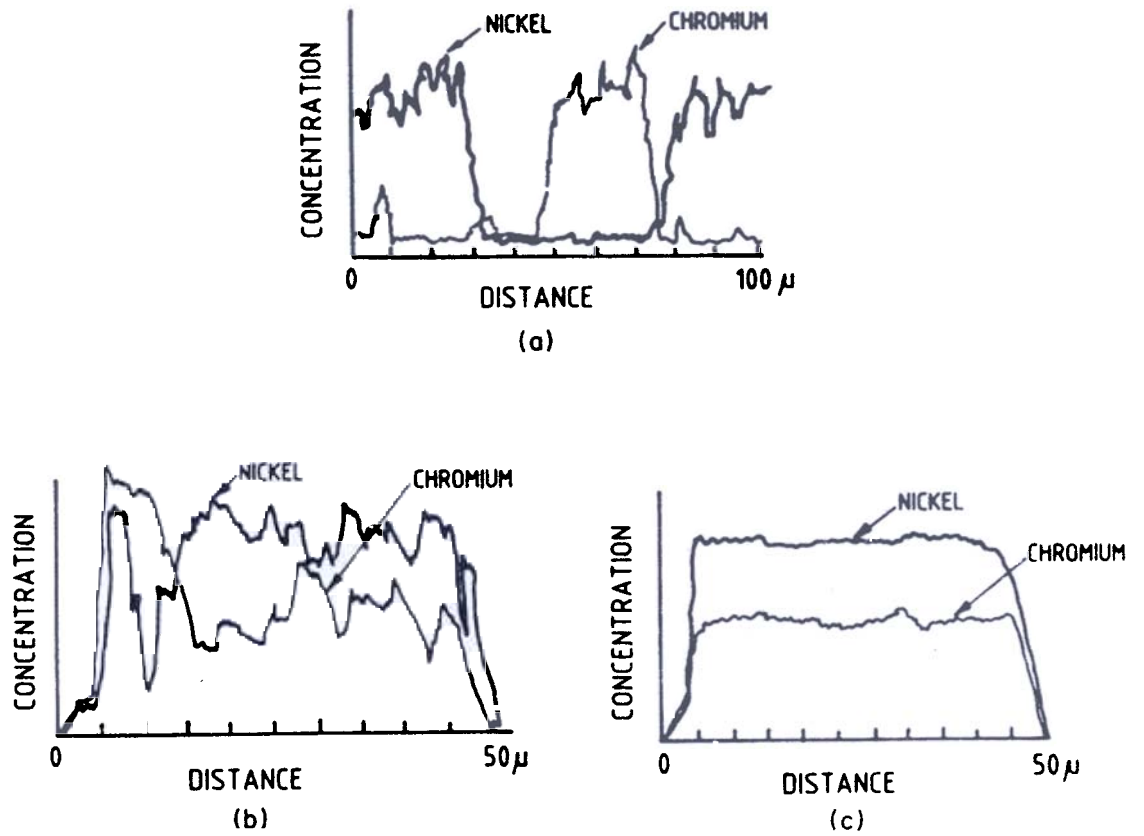
Figure 8. Studies in mechanical alloying – concentration profiles in a particle of a sample : (a) ball-milled for 90 h, (b) attritored for 16 h, and (c) attritored for 40 h.
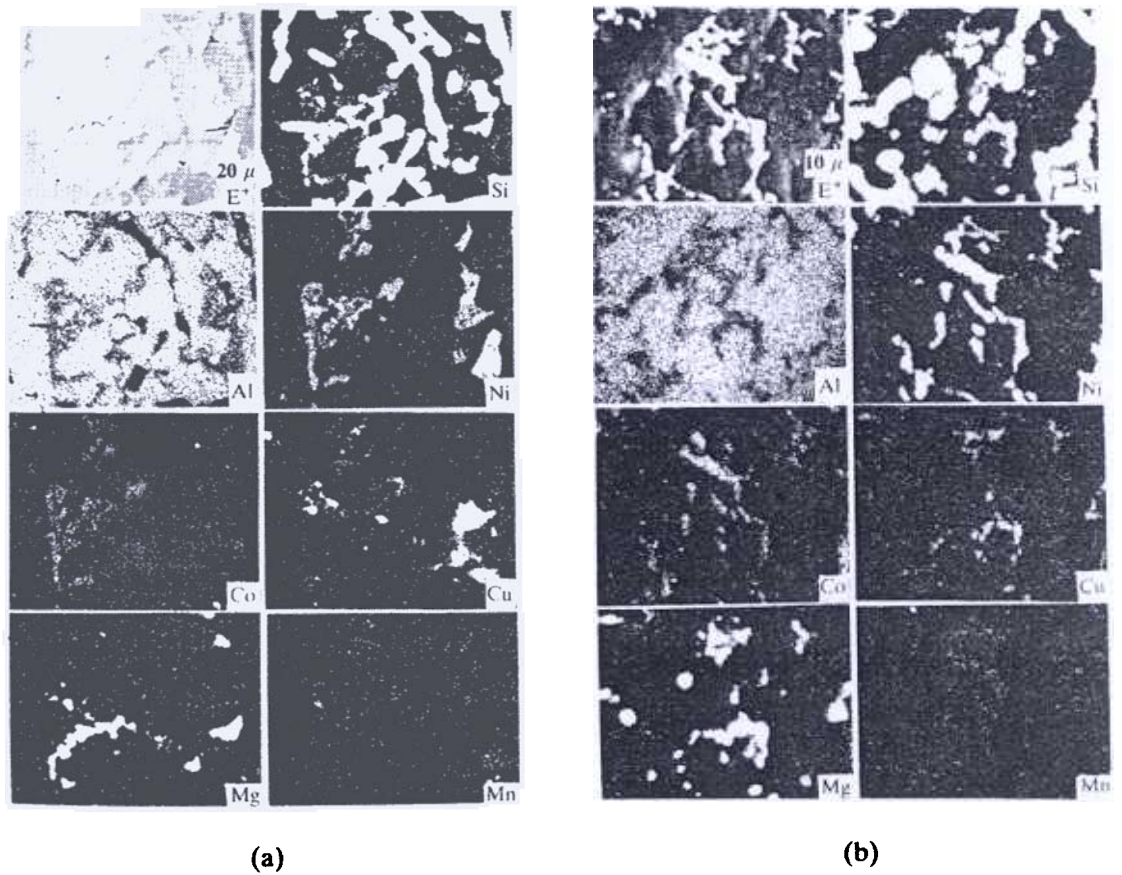

(a)   (b)

Figure 9. X-ray images for an aluminium-silicon alloy : (a) as-cast, (b) liquid-forged.

3.5 Liquid Forging

At DMRL, extensive work has been carried out to develop the liquid metal forging technology so as to manufacture components from ferrous and non-ferrous alloys in a single step from liquid metal to near-net shapes without going through the conventional processes such as casting, forging, etc. During the development work on an aluminium-silicon alloy for producing 'liquid-forged' components, the material has been compared with a conventionally sand-cast alloy component using electron probe microanalyser. The x-ray distribution images taken on a typical area of a liquid-forged sample are shown in Fig. 9(b) while Fig. 9(a) show the x-ray distribution images taken on a typical area of a conventionally-cast sample made from the same alloy. As the magnification of the images taken on the liquid-forged alloy are twice that of the conventionally-cast alloy, it is clear that the liquid forging procedure gives a finer distribution of the elements compared to conventional casting technique, thus leading to better mechanical properties.

3.6 Diffusion Studies

EPMA has found extensive use in binary and ternary diffusion studies. In fact, it is ideally suited for the examination of diffusion samples as the volume of the material analysed is of the order of a cubic micron and the diffusion zone in the
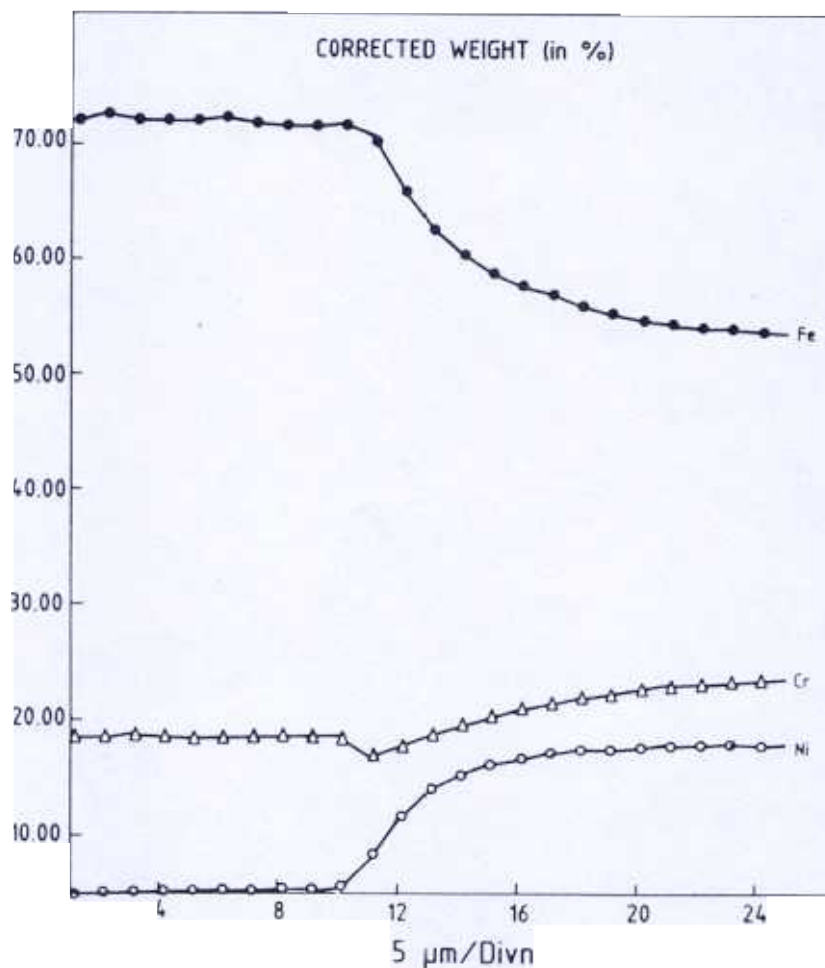

Figure 10. Diffusion studies – concentration profiles.

sample can be transversed in small steps of 5 microns or even less under the electron beam to generate the concentration-distance profiles required for diffusion coefficient calculations. Figure 10 shows the concentrations profiles obtained for an *Fe-Cr-Ni/Fe-Cr* diffusion couple, diffusion-annealed at 1300°C for 48 hours. These profiles have been used to calculate the interdiffusion coefficients.

3.7 EPMA of Nickel-Base Superalloys

Mechanical and creep properties of nickel-base superalloys are strongly dependent on the microstructural features, such as grain size and its distribution, nature of grain boundary precipitates and their distribution, nature and amount of solute elements in the γ matrix as well as on the size, distribution and volume fraction of the coherent intermetallic precipitate, γ'. With the help of optical metallography, general microstructural features such as grain size and approximate volume fraction of γ' can be determined, but for precise investigation, other high resolution techniques are essential. EPMA technique has been found to be very helpful in examining such features, in particular the partitioning behaviour of solute elements between the matrix and γ' or the precipitating carbides/borides phases. Most of the advanced nickel-base superalloys contain elements like *Mo, W, Hf, Nb, B, Zr*, etc., besides conventional *Cr, Co, Ti* and *Al*. These elements not only strengthen the solid solution but have
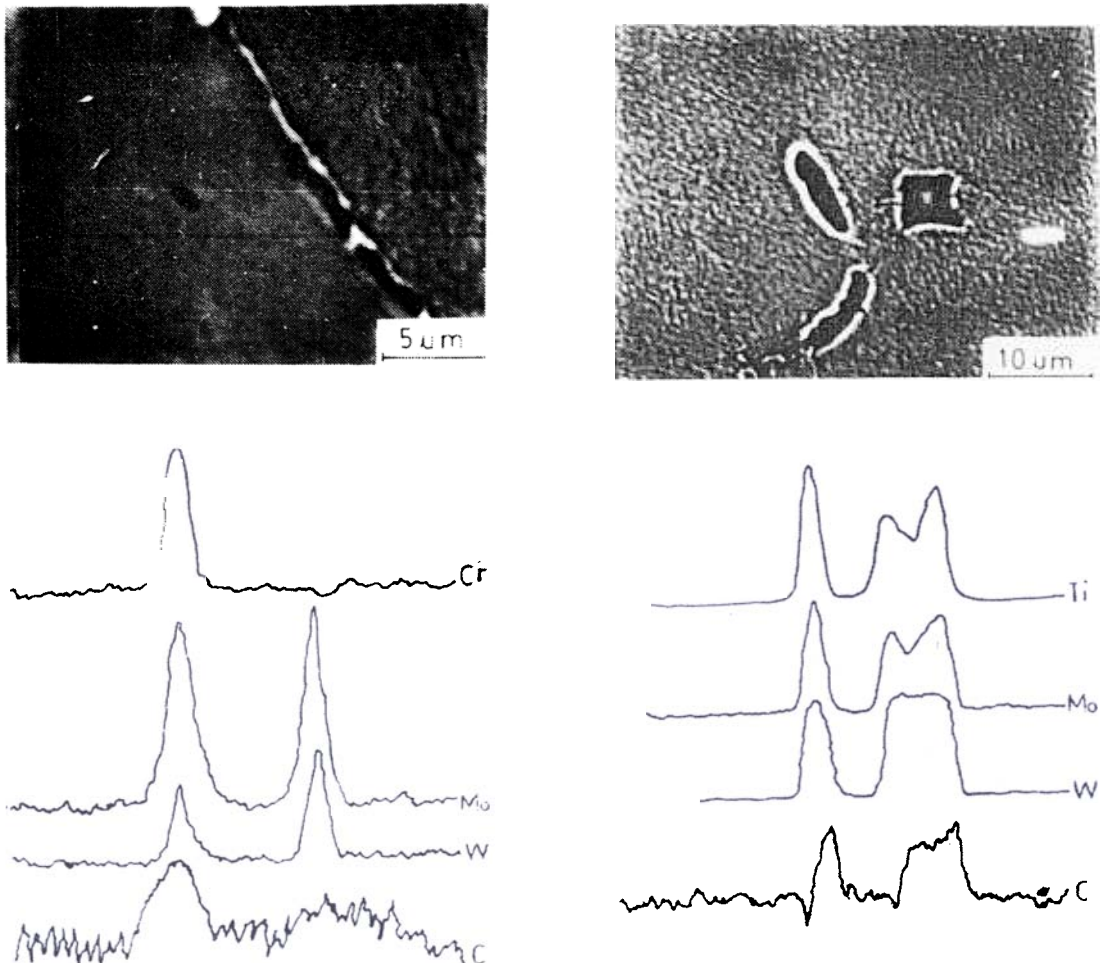

Figure 11　Grain boundary precipitates : Ni-base superalloys – wrought.

also been found to be present in γ' as well as in the inter and intragranular carbides and borides. During heat treatments which include solutionising and aging steps, precipitation reactions take place between these phases and hence it is essential to distinguish and analyse these phases with a view to examine their influence on the short term as well as long term mechanical properties. For example, the information that the carbides are rich in *Mo* and *W* or in *Cr*, would indicate the type of carbides. Similarly, a clear distinction between carbides and borides distributed at the grain boundaries would help in establishing their role in the high temperature properties of these superalloys. In the case of powder metallurgical superalloys, complex oxides, sulphides and nitrides have also been found to be present and their distribution and amount is very critical. EPMA technique has been found particularly useful in analysing such precipitates. Figures 11 and 12 show the linescans for the superalloys, wrought and made by powder metallurgy route respectively, indicating the enrichment of various elements in the grain boundary precipitates. A quantitative analysis of the precipitates would certainly have helped in their accurate identification. However, since their particle size is in the range of the x-ray resolution limit, quantitative analysis is not possible. Linescans on the other hand, are able to illustrate clearly though in a qualitative manner, the partitioning behaviour of various carbide/boride/oxide-forming elements. From this information, it is possible to deduce the nature of precipitates.
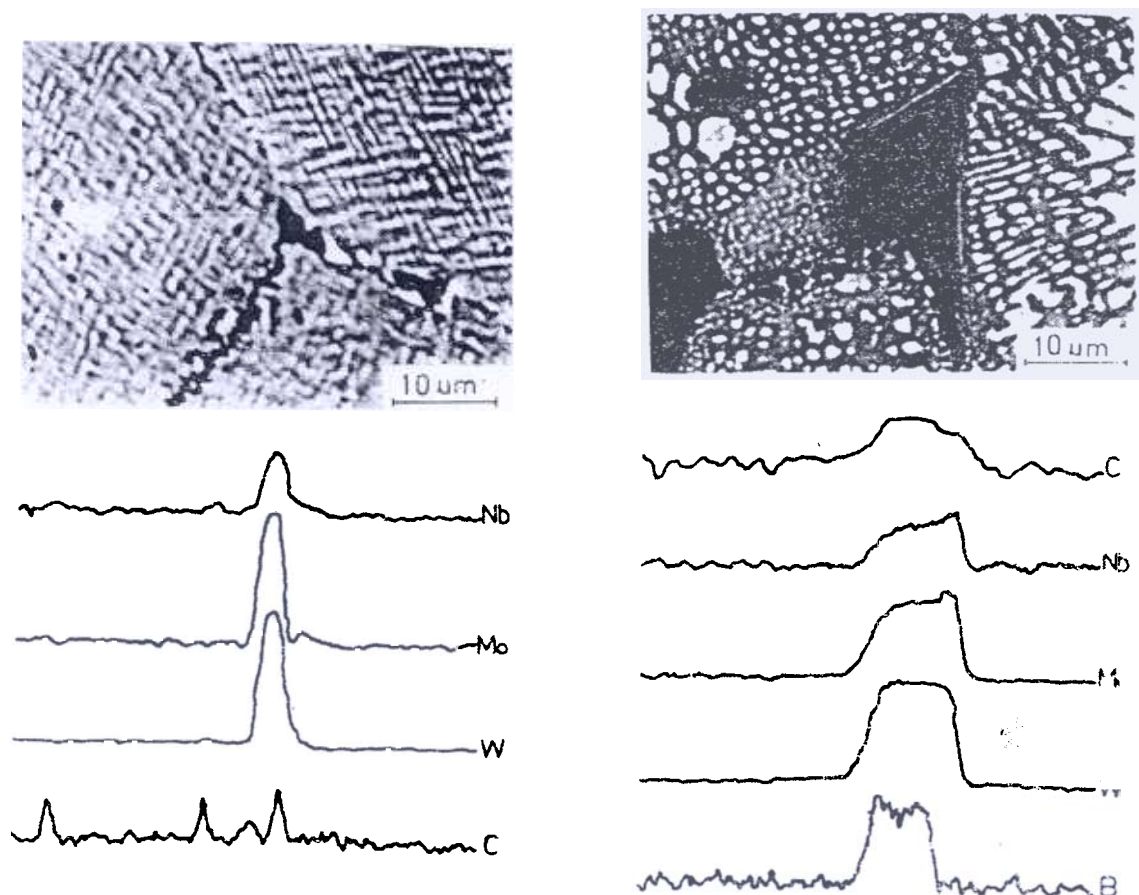

Figure 12. Grain boundary precipitates : Ni-base superalloys – by powder metallurgy route.

4. CONCLUSION

Thus, it is clear that apart from chemical identification of specific microfeatures present in a material, electron probe microanalysis technique can be very gainfully employed to understand how various elements are distributed in a given region of interest, or to illustrate the variation of concentration of various constituent elements across an interface in a coated/welded material, or to examine the products of degradation of a material on corrosion, or to investigate the microchemical changes occurring in a material on failure during service. In short, it can be said that the technique of electron probe microanalysis with its unique lateral and depth resolution can be a very valuable tool in solving many a basic and applied problems in materials research programmes.

ACKNOWLEDGEMENTS

REFERENCES

1   Moseley, H., *Philosophical Magazine,* **26** (1913), 1024

2   Castaing, R. & Guinier, A., *In* Proc. of the First Int Conf. on Electron Microscopy, Delft, 1949.

3. Castaing, R., Ph.D Thesis, University of Paris, 1951.

4. Cosslett, V.E. & Duncumb, P., *Nature,* **177** (1956), 1172.

5. Love, G. & Scott, V.D., *Scanning,* **4** (1981), 111–130.

6. Bastin, G.F., Heijligers, H.J.M. & van Loo, F.J.J., *Scanning,* **6** (1984), 58–68.

BIBLIOGRAPHY

1   Beaman, D.R. & Isasi, J.A., Electron Beam Microanalysis, ASTM–STP-506 (ASTM, Philadelphia), 1972.

2   Belk, J.A.(Ed), Electron Microscopy and Microanalysis of Crystalline Materials (Applied Science Publishers, London), 1970, Chapters 6–8.

3   Bertin, E.P., Introduction to X-ray Spectrometric Analysis, (Plenum Press New York), 1978, Chapter 11.

4   Tousimis, A.J. & Martin, L. (Eds), Electron Probe Microanalysis, (Academic Press, New York), 1969.

5   Anderson, C.A.(Ed), Microprobe Analysis, (Wiley Interscience, New York), 1973.

6. Heinrich, K.F.J., Electron Beam X-ray Microanalysis, (Van Nostrand Reinhold Co., New York), 1981.

7. Poole, D.M. & Martin, P.M., *Metallurgical Reviews,* **14** (1969), 61

8. Martin, P.M. & Poole, D.M., *Metallurgical Reviews,* **15** (1971), 19–46.

9. McKinley, T.D., Heinrich, K.F.J. & Wittry, D.B.(Eds), The Electron Microprobe, (John Wiley, New York), 1966.

10. Scott, V.D. & Love, G., Quantitative Electron Probe Microanalysis, (Ellis Harwood Ltd., Chichester), 1983.

APPENDIX A

APPROXIMATE IDENTIFICATION OF THE SPECIMEN

NEW ACQUISITION BY WDS-SCANNING? Y
ENTER SPEED OF SCANNING (H,M OR L)? M
FIRST IDENTIFICATION LEVEL (High OR Low)? H

SPECTR. NO.   &   XTAL

SYMB	LAMBDA	SIN(A)	C/S
W Yb	1.473	0.36594	440.
NiKB	1.498	0.37203	2999.
CoLu	1.620	0.40228	652.
NiKA	1.658	0.41172	18502.
CoKA	1.789	0.44428	3643.
FeKA	1.937	0.48105	210.
CrKB	2.084	0.51756	426.
CrKA	2.290	0.56873	2598.
TiKA	2.749	0.68263	263
2NiK	2.999	0.74486	176.

SPECTR. NO.   2   &   XTAL   TAP

SYMB	LAMBDA	SIN(A)	C/S
SiKB	6.751	0.26280	1033
W MA	6.979	0.27167	2176
SiKA	7.129	0.27751	423.
AlKA	8.335	0.32447	4186
2SiK	13.482	0.52482	146.
NiLA	14.545	0.56617	465.
2AlK	16.650	0.64813	230.

SPECTR. NO.   3   &   XTAL

SYMB	LAMBDA	SIN(A)	C/S
PmLB	2.083	0.23807	3388.
CrKA	2.291	0.26191	23383.

VKA	2.502	0.28596	1016.
TiKB	2.510	0.28694	1266.
TiKA	2.751	0.31443	3903.
TeLA	3.315	0.37891	2968.
2CoK	3.574	0.40850	781.
2CrK	4.578	0.52330	818.
3NiK	4.974	0.56849	344.
BiMA	5.177	0.59178	356.
MoLA	5.406	0.61794	748.
	6.629	0.75776	232.
WMA	6.981	0.79799	176.

DO YOU WANT A NEW HIGHER LEVEL IDENTIFICATION? N

APPENDIX B

QUALITATIVE CHECK

DESCRIPTION? Y

ENTER ELEMENTS (EXAMPLE : CU RETURN)

EL.NB 1 : AL
EL.NB 2 : CO
EL.NB 3 : CR
EL.NB 4 : MG
EL.NB 5 : MO
EL.NB 6 : NI
EL.NB 7 : SI
EL.NB 8 : TI
EL.NB 9 : W
EL.NB 10 :

ELEM	LINE	SP	POSIT.	PEAK	BG	PEAK-BG
AL	KA	2	32478.	1546.	137.	1409.
AL	KB	2	31001.	112.	89.	23.

ELEM	LINE	SP	POSIT.	PEAK	BG	PEAK-BG
CO	KA	1	44438.	1491.	75.	1416.
CO	LA	2	62235.	18.	8.	10.
CO	KB		40260.	278.	54.	224.
CO	LB	2	60917.	9.	17.	–8.

ELEM	LINE	SP	POSIT.	PEAK	BG	PEAK-BG
CR	KA	1	56867.	1031.	47.	984.
CR	KA	3	26172.	8884.	679.	8205.
CR	KB	1	51793.	204.	34.	170.
CR	KB	3	23837.	1647.	616.	1031.

ELEM	LINE	SP	POSIT.	PEAK	BG	PEAK-BG
MG	KA	2	38506.	40.	72.	–32.
MG	KB	2	37067.	41.	32.	9.

ELEM	LINE	SP	POSIT.	PEAK	BG	PEAK-BG
MO	LA	3	61836.	217.	40.	177.
MO	LB	3	59245.	76.	25.	51.

ELEM	LINE	SP	POSIT.	PEAK	BG	PEAK-BG
NI	KA	1	41183.	6651.	242.	6409.
NI	LA	2	56694.	220.	60.	160.
NI	KB	1	37255.	1051.	68.	983.
NI	LB	2	55462.	42.	42.	0

ELEM	LINE	SP	POSIT.	PEAK	BG	PEAK-BG
SI	KA	2	27751.	295.	146.	149.
SI	KA	3	81487.	12.	11.	
SI	KB	2	26289.	483.	176.	307.
SI	KB	3	77195.	52.	15.	37.

ELEM	LINE	SP	POSIT.	PEAK	BG	PEAK-BG
TI	KA	1	68250.	84.	5.	79.
TI	KA	3	31412.	1653.	282.	1371.
TI	KB	1	62439.	34.	9.	25.
TI	KB	3	28737.	560.	306.	254.

ELEM	LINE	SP	POSIT.	PEAK	BG	PEAK-BG
W	LA	1	36669.	172.	82.	90.
W	MA	2	27185.	785.	197.	588.
W	MA	3	79827.	70.	14.	56.
W	LB	1	31847.	73.	48.	25.
W	MB	2	26294.	482.	154.	328.
W	MB	3	77210.	56.	12.	44.

APPENDIX C

QUANTITATIVE MICROPROBE ANALYSIS

3 ELEMENTS ARE ANALYSED AT 20.00 KV

THE COSECANT OF THE TAKE OFF ANGLE IS 1.556

1TH	STANDARD	IS	PURE	FE	LINE : KA
2TH	STANDARD	IS	PURE	CR	LINE : KA
3TH	STANDARD	IS	PURE	CO	LINE : KA

STD. DATA FOR COUNTING TIME = 10.0 SEC

ELEM	LINE	SPC.	POSITION	(PK-BG)C/S	C = W.F.	+- SIGMA
FE	KA	3	48139.	22455.58	1.00000	0.00211
CR	KA	3	56932.	16804.68	1.00000	0.00244
CO	KA	3	44486.	23710.00	1.00000	0.00205

Normalised '2*Sigma' (Estimation for C. Total = 100%) = 2*(Sum(Sigma)/Sum(C.Exp)) = 0.44 % with averages? Y

M Vijayakumar, et al

FINAL RESULTS

CORRECTED ATOMIC CONCENTRATION %

No.	FE	CR	CO	TOT	+−
	53.545	31.924	14.531	100.000	0.371
2	54.498	30.848	14.653	100.000	0.370
3	53.727	31.525	14.748	100.000	0.372
4	54.684	30.657	14.658	100.000	0.370
5	53.327	32.159	14.514	100.000	0.371
6	54.566	30.891	14.543	100.000	0.370
7	53.556	31.916	14.528	100.000	0.372
average					
	53.986	31.417	14.597	100.000	0.371

CORRECTED WEIGHT FRACTION %

No.	FE	CR	CO	TOT	+−
	54.234	30.106	15.532	99.872	0.370
2	55.194	29.088	15.660	99.942	0.370
3	54.110	29.560	15.674	99.345	0.369
4	55.482	28.960	15.694	100.137	0.370
5	54.075	30.361	15.531	99.968	0.371
6	55.247	29.120	15.538	99.904	0.369
7	54.109	30.022	15.488	99.619	0.370
average					
	54.636	29.602	15.588	99.827	0.370